

BEAM HEAD EROSION IN SELF-IONIZED PLASMA WAKEFIELD ACCELERATORS*

M. Zhou[†], C. E. Clayton, C. Huang, C. Joshi, W. Lu, K. A. Marsh, W. B. Mori (UCLA, Los Angeles, CA 90095) T. Katsouleas, P. Muggli, E. Oz (USC, Los Angeles, CA 90089) M. Berry, I. Blumenfeld, F.-J. Decker, M. J. Hogan, R. Ischebeck, R. Iverson, N. Kirby, R. Siemann, D. Walz (SLAC, Menlo Park, CA 94025)

Abstract

In the recent plasma wakefield accelerator experiments at SLAC, the energy of the particles in the tail of the 42 GeV electron beam were doubled in less than one meter [1]. Simulations suggest that the acceleration length was limited by a new phenomenon – beam head erosion in self-ionized plasmas. In vacuum, a particle beam expands transversely in a distance given by β^* . In the blowout regime of a plasma wakefield [2], the majority of the beam is focused by the ion channel, while the beam head slowly spreads since it takes a finite time for the ion channel to form. It is observed that in self-ionized plasmas, the head spreading is exacerbated compared to that in pre-ionized plasmas, causing the ionization front to move backward (erode). A simple theoretical model is used to estimate the upper limit of the erosion rate for a bi-gaussian beam by assuming free expansion of the beam head before the ionization front. Comparison with simulations suggests that half this maximum value can serve as an estimate for the erosion rate. Critical parameters to the erosion rate are discussed.

INTRODUCTION

In current frontier of the plasma wakefield accelerator (PWFA) [3] experiments, the plasmas are generated via field-ionization of neutral gases by the particle beam space charge (self-ionized). This self-ionized regime has made meter-long, high-density ($> 10^{16} \text{cm}^{-3}$) plasma sources possible, which is desirable by future afterburner designs [4]. In the recent years, the energy gain achieved in the experiments has been increased from a few GeV to ~40 GeV by lengthening the plasma source (from ~10cm to ~90cm) [1,5,6]. However, the increasing trend stopped beyond ~100cm for these parameters in the most recent experiment [1]. Detailed Particle in Cell (PIC) simulations modeling these experiments suggest that a new phenomena – beam head erosion in self-ionized plasmas – is the major factor that limited further energy gain.

* Work supported by Department of Energy contracts DE-AC02-76SF00515, DE-FG02-92ER40727, DE-FG02-92-ER40745 DE-FG02-03ER54721, DE-FC02-01ER41179 and NSF grant Phy-0321345

[†] mmzhou@ee.ucla.edu

RECESSION OF THE IONIZATION FRONT -- SIMULATION OBSERVATIONS

Some properties of the self-ionized regime (e.g. wake excitation and hosing instability) have been previously studied using PIC simulations [7,8,9]. Here we use a novel 3D quasi-static PIC code, QuickPIC [10] to study the head erosion. QuickPIC is fully relativistic, fully nonlinear and fully parallelized. It models the field-ionization process using the ADK model [11,12] and the energy loss effects from synchrotron radiation through an effective drag force [13].

After a systematic parameter scan (i.e. varying the beam charge/emittance/size and plasma density etc. in a large range), it is observed that the wake front erodes back faster in a self-ionized plasma than in a pre-ionized plasma in otherwise identical conditions. Here, the wake front is defined as the ionization front in a self-ionized case and the perturbation front (e.g. 3% of plasma electron density drop) in a pre-ionized case.

Figure 1 is an example showing the beam/wake erosion. In this simulation, there are 1.8×10^{10} electrons in the 28.5 GeV beam. The beam is bi-gaussian with $\sigma_r = 7 \mu\text{m}$ and $\sigma_z = 45 \mu\text{m}$, and has a normalized emittance of $15 \text{mm} \cdot \text{mrad}$. The neutral lithium density is $2 \times 10^{16} \text{cm}^{-3}$. We can see that in the pre-ionized case, the wake front has barely moved in the 300 centimeter propagation distance while in the self-ionized case, the wake front has eroded back so much that at $s = 300\text{cm}$, the beam has become too dispersed to be seen (in this color table) and is no longer able to ionize the neutral lithium gas.

A convergence test suggests that resolving the betatron oscillation is necessary for correctly modeling the erosion process. In the test, updating the electron beam in a distance so that there are 10 steps per betatron oscillation for particles inside the ion channel gives almost identical erosion results to that of 40 steps per oscillation. While under-resolving the betatron oscillation (e.g. 2.5 steps per oscillation) gives spuriously higher erosion rate.

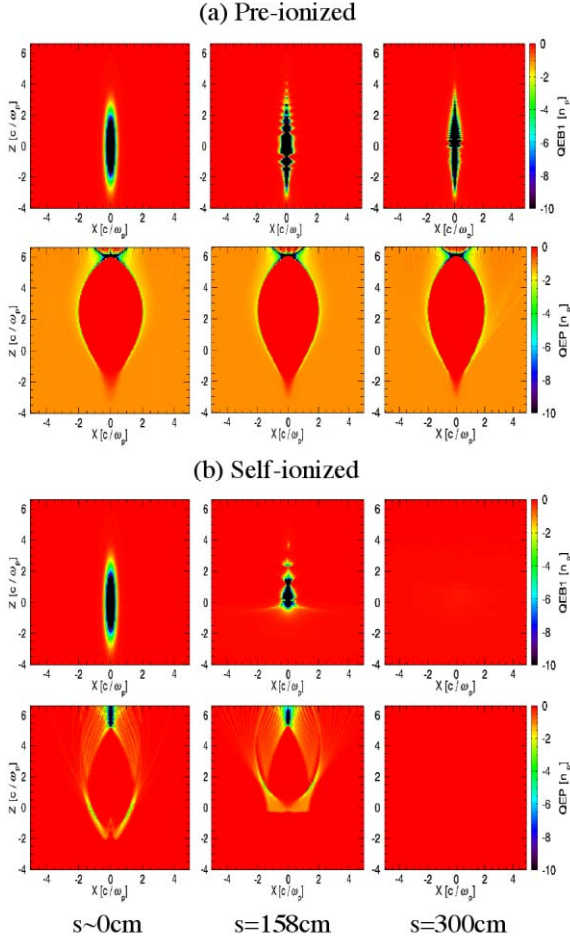


Figure 1. Beam (top) and plasma (bottom) densities at 3 different locations ($s \sim 0\text{cm}$, 158cm and 300cm along the plasma) in (a) pre-ionized and (b) self-ionized plasmas

UPPER LIMIT OF THE EROSION RATE FOR A BI-GAUSSIAN BEAM – THEORETICAL MODEL

In this section, we estimate the erosion rate in a self-ionized plasma generated by a bi-gaussian beam using a simple theoretical model. Figure 2 shows the schematic of the beam head evolution. Due to the electric field from a relativistic bi-gaussian beam

$$E_r(r, \xi) = 22960 \left(\frac{N}{2 \times 10^{10}} \right) \frac{1}{\sigma_z(\mu\text{m})r(\mu\text{m})} e^{-\frac{r^2}{2\sigma_z^2}} (1 - e^{-\frac{r^2}{2\sigma_r^2}}) (GV/m)$$

, there is a ‘W’ shaped ionization front. At $s = 0$, the ionization front is at A and the ion channel is completely formed at B. If the beam has a finite emittance, the part before A will undergo vacuum expansion while that between A and B will expand at a lower rate. This spot-size increase will lead to a later ionization front at location $s + \Delta s$. Next, we calculate the head erosion rate, which is defined as the rate of the moving ionization front A.

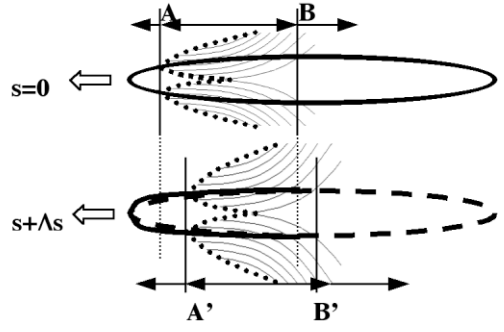


Figure 2. Schematic of the ionization front recession

For simplicity, we assume that at a certain location s , the part of the beam before the ionization front has freely expanded just like in vacuum due to its finite emittance (i.e. $\sigma_r(s) = \sigma_{r0} \sqrt{1 + \frac{(s-s_0)^2}{\beta^{*2}}}$, where s_0 and σ_{r0} are the location and spotsize at waist, and β^* is the beam function ($\beta^* = \frac{\gamma \sigma_{r0}^2}{\epsilon_n}$). By equaling the ionization threshold field E_{th} and the maximum space charge field E_r at a certain slice ξ ,

$$E_{r\max}(\xi, s) = 10360 \times \frac{N}{2 \times 10^{10}} \times e^{-\frac{\xi^2}{2\sigma_z^2}} \times \frac{1}{\sigma_z(\mu\text{m})\sigma_r(\xi, s)(\mu\text{m})} (GV/m),$$

we can get the location of the ionization front ξ_{ion} as a function of s , $\xi_{ion}(s) = \sqrt{\xi_{ion}^2(s=s_0) - \sigma_z^2 \cdot \ln(1 + \frac{(s-s_0)^2}{\beta^{*2}})}$ or

$$\xi_{ion}(s) / \sigma_z = \sqrt{-2 \ln \left[\frac{E_{th}(GV/m)\sigma_z(\mu\text{m})\sigma_{r0}(\mu\text{m})}{10360 \times \frac{N}{2 \times 10^{10}}} \right] - \ln(1 + \frac{(s-s_0)^2}{\beta^{*2}})} \quad (\text{eq. 1})$$

Figure 3 plots the evolution of ξ_{ion} as a function of propagation distance s for several different initial ionization front locations ($\xi_{i0} \equiv \xi_{ion}(s=s_0) = 0.5 \sim 4\sigma_z$). Since the expansion rate for the beam part between A and B is actually smaller than the vacuum expansion rate, Equation 1 gives an upper limit for the head erosion rate.

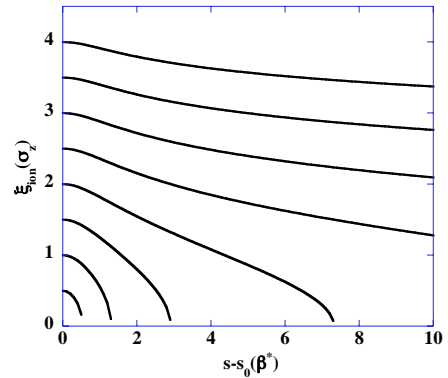


Figure 3. Evolution of the ionization front location (in unit of σ_z ahead of beam center)

Figure 3 indicates that the head erosion of a bi-gaussian beam depends on both the beam β^* (2nd term in eq. 1) and the initial ionization front location (1st term in eq. 1). The latter depends on the number of electrons in the beam (N), the beam size (σ_{r0}, σ_z) and the type of the neutral gas (E_{th}). These are important parameters to monitor in future afterburner relevant experiments to prevent head erosion from becoming detrimental. For example, in the SLAC experiments, this can be overcome by getting rid of the foil spoiling so as to preserve the beam emittance.

EROSION RATE FOR BI-GAUSSIAN BEAMS – SIMULATION RESULTS

Simulations are performed to compare with the vacuum expansion model described in the previous section. In these simulations, the 28.5 GeV beams have 1.8×10^{10} electrons and the neutral lithium densities are $2 \times 10^{16} \text{ cm}^{-3}$. The beam parameters are chosen so that the initial ionization fronts are located at $1.2, 1.7$ and $2.2 \sigma_z$ ahead of the beam center respectively (See Table 1).

	$\sigma_{r0}(\mu\text{m})$	$\sigma_z(\mu\text{m})$	ϵ_n (mm·mrad)	$\beta^*(\text{cm})$	$\xi_{i0}(\sigma_z)$
(a)	15	45	95	13	1.2
(b)	7	45	15	18	1.7
(c)	7	15	55	4.9	2.2

Table 1. Beam parameters for head erosion simulations

Figure 4 plots the measured ionization front location from simulations (blue dots) comparing with those calculated from the vacuum expansion model (red line).

In these 3 cases, the upper limit of the erosion rate given by this simple vacuum expansion model is not far above that observed in the simulations (approximately two times larger). This suggests the usefulness of Equation 1 in estimating the actual erosion rate. An improved theoretical model is being developed based on a more systematic study of the erosion rate dependence on beam/plasma parameters.

CONCLUSION

In PIC simulations of the PWFA, exacerbated beam head erosion were observed in self-ionized plasmas than in pre-ionized plasmas. This erosion due to the lack of focusing at the beam head in a self-ionized plasma explains the energy gain saturation observed in the recent energy doubling experiments. Based on a vacuum expansion model, Equation 1 gives the location of the receding ionization front under a largest possible erosion rate. Comparison with simulations suggests that half this value could serve as a rough estimate of the actual erosion rate. Minimizing the beam emittance can slow down the head erosion process. Other possible solutions such as using external focusing or partially pre-ionized plasma to confine the beam head also need to be explored.

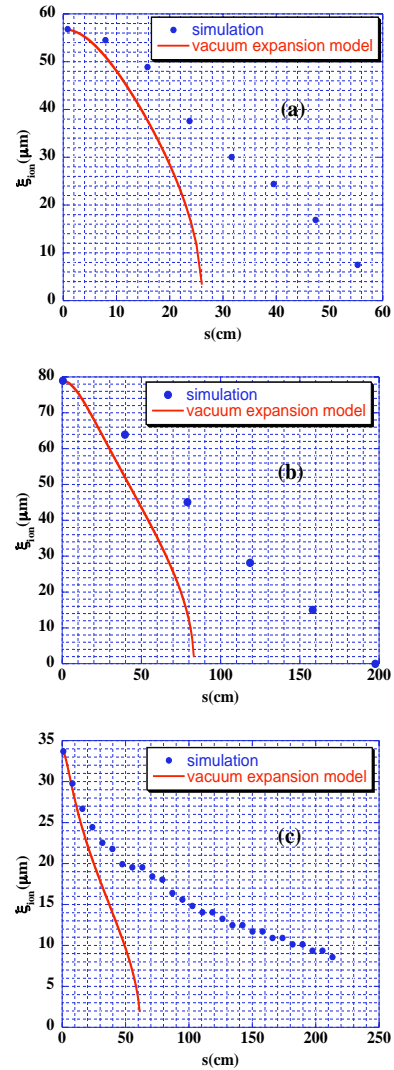


Figure 4. Ionization front location evolution for initial locations ξ_{i0} at (a) $1.2 \sigma_z$ (b) $1.7 \sigma_z$ and (c) $2.2 \sigma_z$

REFERENCES

- [1] I. Blumenfeld *et al.*, Nature **445**, 741(2007)
- [2] J. B. Rosenzweig *et al.*, Phys. Rev. A **44**, R6189 (1991)
- [3] T. Tajima and J. M. Dawson, Phys. Rev. Lett. **43**, 267 (1979)
- [4] S. Lee *et al.*, Phys. Rev. S. T. AB **5**, 011001(2002)
- [5] M. J. Hogan *et al.*, Phys. Rev. Lett. **95**, 054802 (2005)
- [6] P. Muggli *et al.*, these proceedings. (2007)
- [7] D. L. Bruhwiler *et al.*, Phys. Plasmas **10**, 2022(2003)
- [8] S. Deng *et al.*, Phys. Rev. E **68**, 047401(2003)
- [9] S. Deng *et al.*, Phys. Rev. Lett. **96**, 045001 (2006)
- [10] C. Huang *et al.*, J. Comput. Phys. **217**, 658 (2006)
- [11] M. V. Ammosov *et al.*, Sov. Phys. JETP **64** (6), 1191 (1986)
- [12] M. Zhou *et al.*, PAC'05, Knoxville, TN, May 2005, p. 2905
- [13] Based on the relativistic Lamor formula.